JOURNAL OF APPLIED ELECTROCHEMISTRY 5 (1975) 129–135

Electrodeposition from a fluidized bed electrolyte. II. Effects of bed porosity and particle size

D. C. CARBIN

Torday Ltd, North Shields

D. R. GABE

Department of Materials Technology, Loughborough University of Technology

Received 2 June 1974

Mass transfer from a fluidized bed electrolyte containing inert particles has been found to depend on bed porosity and particle size. The optimum porosity was found to vary from 0·52 − 0·57 with decreasing particle size but mass transport increased with particle size.

A mass transfer entry length effect was observed on the cylindrical cathode but its position within the bulk of the bed was found not to be critical, thus indicating that the hydrodynamic entry length was small. The limiting current density was found to vary as $(d_e/L_e)^{0.15}$ where d_e is the annular equivalent diameter and L_e the electrode length.

List of symbols

Re_I = modified Reynolds No. $= U_0 d_p/\nu(1-\epsilon)$
Re_{II} = particle Reynolds No. $= U_0 d_p/\nu$
Re_0 = sedimentation Reynolds No. $= U_i d_p/\nu$ (constant value)
Re_t = terminal particle Reynolds No. $= U_t d_p/\nu$
Sc = Schmidt No. $= \nu/D$
St_I = modified Stanton No. $= k_L \epsilon/U_0$
C_b = bulk concentration, M cm^{-3}
D = diffusion coefficient, cm^2 s^{-1}
d_t = tube diameter, mm
d_e = electrode equivalent diameter, mm
d_p = particle diameter, mm
ϵ = bed porosity
zF = Faradaic equivalence
cd = current density
i_L = limiting current density, mA cm^{-2}
i_{L0} = limiting current density in the absence of particles
k_L = mass transfer coefficient, cm s^{-1}
L_e = electrode length, mm
m, n = constants or indices
ν = kinematic viscosity, cm^2 s^{-1}
U_0 = superficial velocity, cm s^{-1}
U_i = sedimentation velocity, cm s^{-1}

1. Introduction

The fluidized bed reactor is finding increasing application as a convenient means of increasing mass transport and hence total reaction during electrochemical operations. In particular, electrodeposition of metal from waste and leach liquors is an attractive proposition in the aim of process economy. While the best known and most well developed form of the fluidized bed reactor makes use of active or conducting metal particles in the bed, thereby providing very large electrode surface areas, this very feature makes the bed less susceptible to detailed mass transfer analysis. In particular, bed porosity and particle size must necessarily be important variables but with an active or growing particle, optimal conditions may change during a process cycle as far as fluid stability is concerned. For this reason, it was decided to examine the effects of bed porosity and particle size during electrodeposition from an electrolyte containing non-conducting stable particles and thereby consider their effect on diffusion-layer thickness and eliminate any uncertainty in the value of electrode surface area.

In a previous investigation [1] the mass transfer behaviour has been described by a dimensionless

correlation of the form:

$$St_I = 1{\cdot}24\, Sc^{-0{\cdot}67}\, Re_I^{-0{\cdot}57}. \qquad (1)$$

Work reported by other workers on the same type of inert particle bed has indicated that an optimum bed porosity exists for maximum mass transport and this has been further investigated in this research.

2. Experimental

The fluidization cell consisted of a perspex tube, 31·7 mm in diameter, closed at the bottom end with a *Vyon* filter capable of supporting the bed of ballotini glass beads (184, 261 and 354 μm mean diameter). Copper sulphate electrolyte (0·005, 0·015 and 0·07 M containing 0·5 M H_2SO_4) was used to fluidize the bed, flow rates of 0–15 mm s^{-1} being achieved by means of a peristaltic pump giving bed expansions of 0·05–3·0. Cylindrical copper cathodes (6.32 mm diameter) were suspended in the bed from 5·3–48·2 mm above the supporting membrane (20 mm being regarded as a 'norm'). Full details have been reported elsewhere [1]. Limiting current density values were obtained using a potentiokinetic technique (100 mV min^{-1}) and a potentiometric recorder.

3. Results

The limiting cd values reported previously were obtained as constant current portions of the potential-current polarization curves and except when the bed expansion was very low (< 0·2) the value was clearly defined. At low bed expansions the reproducibility was low but the variation of limiting cd i_L with bed expansion may be seen in Fig. 1. Fluidization occurred at a bed porosity of 0·4 [2, 3] and a maximum value of i_L was found over a relatively narrow range of expansion, the exact value varying with particle size. The maximum increase occurred with the largest particle size (354 μm) and the highest temperature investigated. If the limiting cd value is related to the superficial flow velocity (Fig. 2) however, it may be seen that the smallest particle size has a more pronounced effect on i_L at low solution velocities because of the greater extent of bed expansion, but as the velocity is increased and the maximum value of i_L for 184 μm particles is exceeded, the larger particles give higher values. In each case

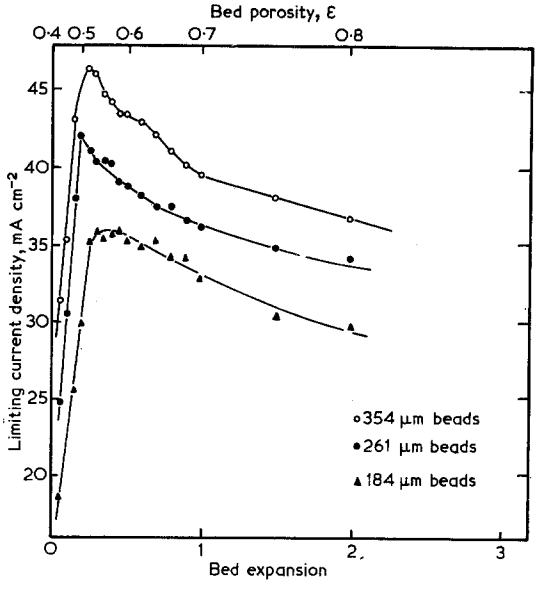

Fig. 1. Effect of bed expansion and porosity on the limiting current density. 0·07 M $CuSO_4$; 21·5° C.

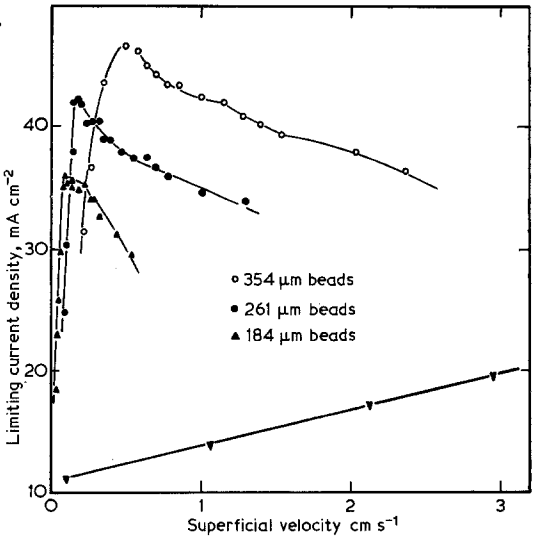

Fig. 2. Effect of flow velocity on the limiting current density. As Fig. 1, but including data in the absence of beads.

and at all velocities examined the limiting cd was well above that obtained in the absence of particles.

Although fluidized beds are thought to exhibit the property of thorough mixing, the extent of a hydrodynamic entry length was investigated by placing the central electrode at various axial heights (0–115 mm) above the bed support membrane in

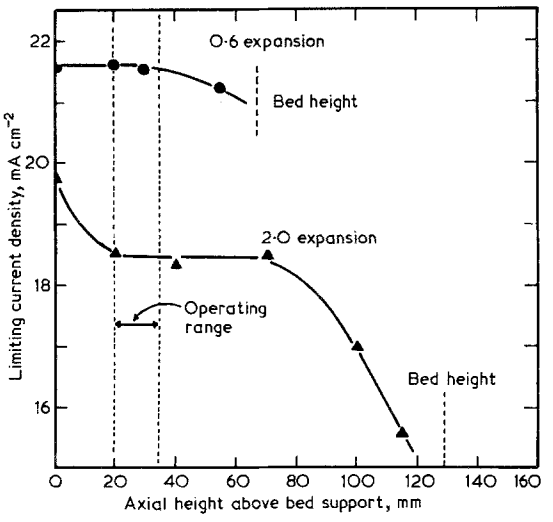

Fig. 3. Effect of axial height in the bed on the *average* limiting current density.

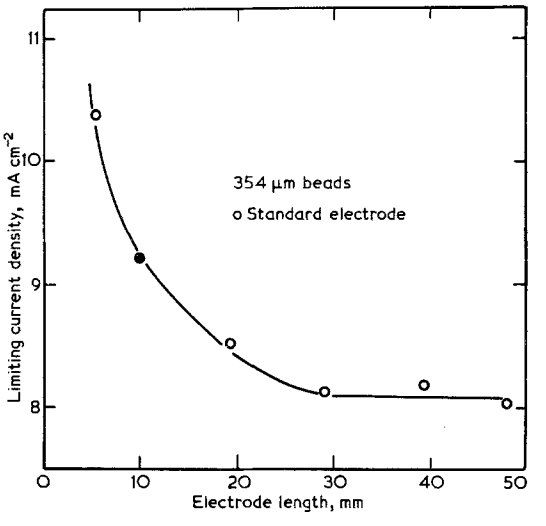

Fig. 4. Effect of electrode length on the *average* limiting current density.
0·015 M $CuSO_4$; 22·8°C: 354 μm beads.

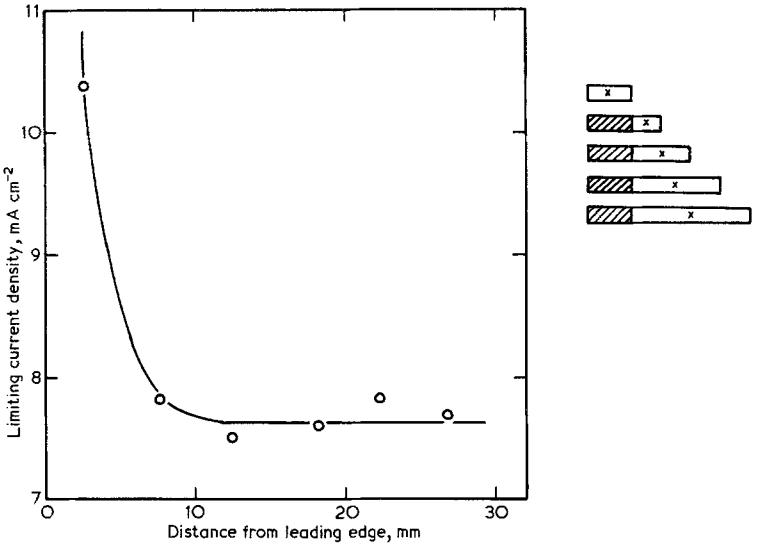

Fig. 5. Variation of the limiting current density with distance from the leading edge.
0·015 M $CuSO_4$; 22·8°C: 354 μm beads.

beds expanded to 0·6 and 2·0. Limiting cd values (Fig. 3) at an expansion of 0·6 were found to be constant for electrodes held up to 40 mm above the membrane but fell for greater heights. For an expansion of 2·0, a bed entrance effect was apparent such that up to 20 mm above the membrane i_L decreased with height, remained constant for heights up to 70 mm, but fell for any greater height. For the complete range of bed expansions (0·05–3·0), therefore, a narrow range of height (20–35 mm) existed above the membrane in which a constant value of i_L was obtained unaffected either by bed hydrodynamic entrance or bed surface segregation effects.

The existence of a mass transfer entry length on the cylindrical electrode was also investigated by means of a series of electrodes of various lengths for which average limiting cd values were measured

(Fig. 4). These values indicated the presence of an entry effect, as in the case of flow in the absence of particles [4], and suggests that a short electrode length of 11 mm might yield i_L values 14% higher than an electrode length of 30 mm. Values of i_L for various points along an electrode of length 48·2 mm were calculated (Fig. 5) and show that the electrode entry length is about 20 mm; when the bed surface effect is also considered, the optimum sample length may be seen to be about 15 mm when placed about 20 mm above the bed support membrane.

4. Discussion

4.1. *Entry length effects*

Although Coeuret *et al.* [2] reported that there was no variation in mass transfer rates for axial heights above the entry region, Jottrand and Grunchard [5] have observed a continuous drop in the mass transfer rate as the upper surface was approached. This was probably due to large segregation effects in the bed due to poor particle size control. In this study, care was taken to ensure a constancy of particle size yet segregation effects were found for the top one-half of the bed, i.e. distances greater than 65 mm above the bed support for a total bed height of 129 mm. The bed entry length might also be due to oversized particles segregating at the bottom but could also be attributed to the distance for hydrodynamic flow conditions to stabilize.

In the absence of fluidized particles mass transfer has been found to vary with the ratio of diameter to length (d_e/L_e) according to a relation of the type:

$$i_L \sim (d_e/L_e)^m. \qquad (2)$$

For an annular system [6, 7] in laminar flow, m has a value of about 1/3 [6, 7]. Insufficient data are available here for a complete analysis because the cathode diameter was maintained constant at 6·32 mm but, assuming a similar behaviour, m = 0·147 (Fig. 6) thereby implying that the correlation obtained previously [1] might be modified to:

$$St_I = 1{\cdot}24Sc^{-0{\cdot}67}Re_I^{-0{\cdot}57}(d_e/L_e)^{0{\cdot}15}. \qquad (3)$$

4.2. *Effect of particle size*

In heat transfer studies it has been proposed that, for a given bed porosity, increasing the particle size results in increased particle momentum and hence increased heat transfer rates [8]. This has not been previously reported as a clear finding for mass transfer. The data of Fig. 2 enable this to be examined by making allowance at all bed expansions for the effect of a flowing electrolyte and then examining the effect of particles *per se*. This has been done in Fig. 7 and a similar behaviour has been

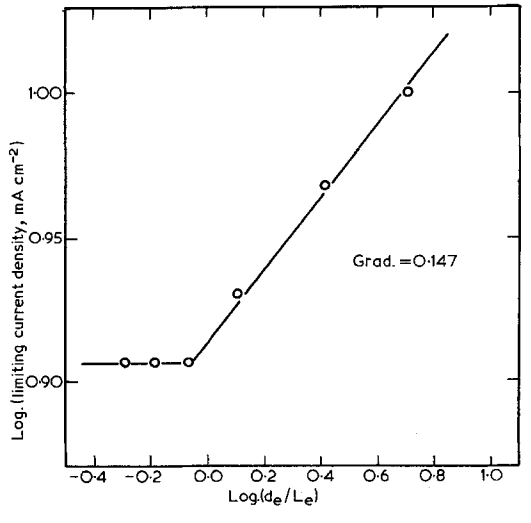

Fig. 6. Relationship between *average* limiting current density and the ratio d_e/L_e.

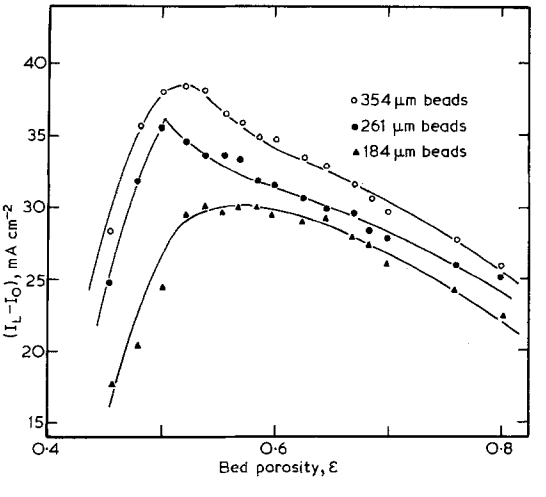

Fig. 7. Effect of particle size on the limiting current density, correcting for the contribution of electrolyte flow. 0·07 M $CuSO_4$; 21·5°C.

found for the more dilute solutions [9]. It is quite clear that the larger particles are more effective at reducing the diffusion layer thickness at all bed expansions. Only Coeuret *et al.* [2] of the earlier investigators have supplied enough data to make a similar analysis possible and by replotting their results (Fig. 8), a similar pattern emerges.

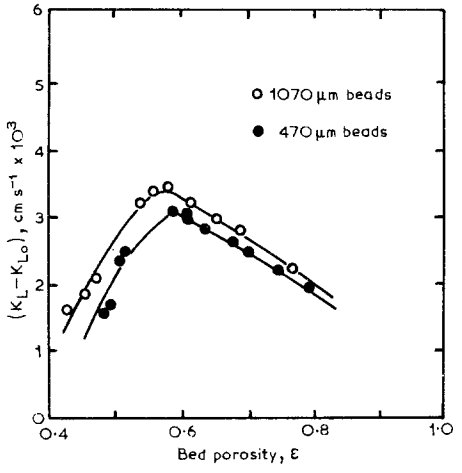

Fig. 8. As Fig. 7, but data from Coeuret *et al.* [2].

When the bed is initially fluidized at low bed expansion, it appears likely that particle agglomeration takes place, with perhaps a common agglomerate size irrespective of particle size. As the bed expands, agglomerates break up and the mass transport maximum may correspond to the existence of individual particles; above the maximum the particles are effectively diluted without any compensating increase in the effective number of individual solid entities. Coeuret *et al.* [2] have shown that the tendency for aggregate formation increases with decreasing particle size thus suggesting that aggregates of particles exist up to large porosities for smaller particles thereby explaining why the maximum in i_L value shifts to higher bed porosities for decreasing particle size.

4.3. *Optimum bed porosity*

A maximum mass transfer rate has been observed over a narrow range of bed porosity and while such maxima have been observed previously [2, 5, 9], they were not quite so pronounced. The values of the optimum porosity ϵ_{opt} have been tabulated in Table I from which it is clear that they decrease

Table 1. Optimum porosities for maximum mass transfer

	Particle Size (μm)	*Optimum bed porosity*
This investigation	185	0·570
	260	0·522
	355	0·516
Jottrand and Grunchard [5]	220	0·58
	340	0·57
	780	0·57
Coeuret *et al.* [2]	350	0·62
	470	0·60
	690	0·60
	980	0·61
	1070	0·56

with increasing particle size for all three sets of data. While the existence of a maximum can be attributed to the optimization of increasing flow, by increasing particle agitation causing increased mass transfer and increasing particle dilution causing decreased mass transfer, no prediction of optimum porosity is forthcoming. Beek [10] and others [8, 11] have suggested that it may be predicted from the empirical mass transfer correlation which was found to be [1]:

$$i_L = 1{\cdot}24FC_b(1-\epsilon)^{0{\cdot}57}\epsilon^{-1{\cdot}0}U_0^{0{\cdot}43}d_p^{-0{\cdot}57}\nu^{-0{\cdot}1}D^{0{\cdot}67}. \quad (4)$$

Here only the terms involving ϵ and U are relevant to a maximization procedure for which we may replace U_0 by a function of ϵ using the relation [11, 12]

$$U_0 = U_i\epsilon^n \quad (5)$$

where U_i is the sedimentation velocity, i.e. the free fall velocity of particles at sedimentation, and n is a constant. However, taking account of the particle diameter d_p we may prefer:

$$Re_{II} = Re_0\epsilon^n \quad (6)$$

where $Re_0 = U_i d_p/\nu$ and is constant for a given particle size and solution. Values of Re_{II} may be plotted against ϵ on a log–log scale (Fig. 9) and the values of n determined are given in Table II.

Richardson and Zaki [11] gave empirical equations to calculate values of n at various values of Re and these are included in Table II for comparison.

The terms in ϵ and U_0 can now be written in the form:

Table 2. Measured and calculated values of n for: $Re_{II} = Re_0^n$

Mean Particle Size (μm)	Temperature 21·5°C		Temperature 40°C	
	Measured value	Calculated value*	Measured value	Calculated value*
184	4·61	3·79	4·76	3·52
261	4·44	3·65	4·38	3·46
354	3·86	3·46	3·79	3·28

* For $1 < Re_t < 200$, Richardson and Zaki [11] give:

$$n = \left(4{\cdot}4 + 18\frac{d_p}{d_t}\right)Re_t^{-0{\cdot}1}$$

d_t is the tube diameter.
d_p is the particle diameter.
Re_t is the terminal particle Reynolds number.

$$f(\epsilon) = \frac{(1-\epsilon)^{0{\cdot}57}}{\epsilon}(\epsilon^{0{\cdot}43\,n}). \qquad (7)$$

Substituting the values for n given in Table II this equation may be plotted graphically as in Fig. 10 from which the maxima in $f(\epsilon)$ appear at bed porosities of 0·52, 0·63 and 0·65 for particle sizes of 354, 261 and 184 μm respectively. Comparing these values with the experimental values in Table I it may be seen that prediction and observation only agree for the 354 μm particles. Part of the discrepancy may be accounted for by the error in predicting Re_t in the region of $Re_{II} = 2{\cdot}0$ by means of either Stokes' or Newton's Laws. Furthermore the particle sizes quoted are mean values for a particular batch.

For heat transfer studies Brea and Hamilton [7] have proposed a similar but rather more extended means of predicting the optimum porosity; selected data subjected to their analysis did not give an improved prediction of the optimum porosity value. This approach clearly has very limited success in this problem; nevertheless it is important to be able to predict the optimum value of bed porosity for any given particle size because the value of i_L is very sensitive to changes in ϵ near the optimum value.

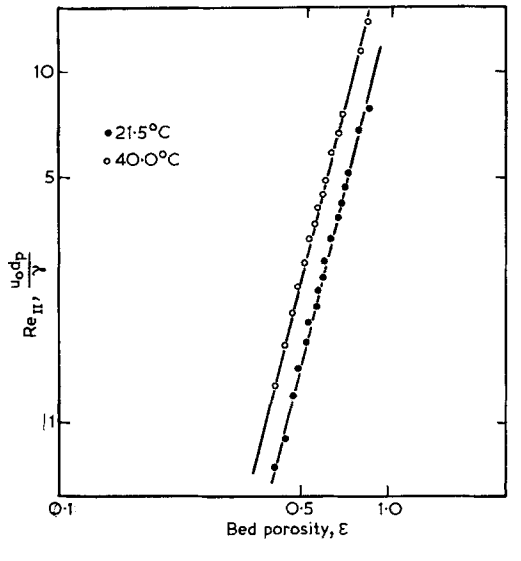

Fig. 9. Variation of the tube Reynolds number with bed porosity.
0·07 M $CuSO_4$; 354 μm beads.

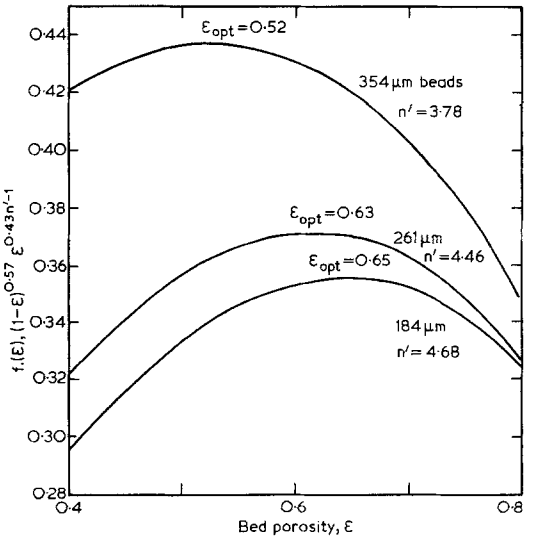

Fig. 10. The optimum bed porosity expressed as maxima for $f(\epsilon)$.

Exploitation of the fluidized bed will involve optimization and for the most economical power consumption some control of the bed at the optimum porosity is desirable. From Fig. 5 it is apparent that compared with a particle-free flowing electrolyte, the limiting cd is always higher but at the optimum porosity an improvement of about four times can be achieved. If the maximum in mass transfer occurs when particles essentially lose contact or coherency with each other it is possible that its importance to a bed of conducting particles is that, at the 'optimum' porosity, electrical continuity through the particles is lost and operation ceases to have the virtue of large active electrode area.

Acknowledgements

The work was carried out in the Metallurgy Department, University of Sheffield.

The authors gratefully acknowledge the provision of laboratory facilities by Professor G. W. Greenwood and the award of a studentship (to D.C.C.) by the Science Research Council.

References

[1] D. C. Carbin and D. R. Gabe, *Electrochim. Acta*, **19**, (1974) 645.
[2] F. Coeuret, P. Le Goff and E. Vergnes, *Proc. Int. Symp. Fluidisation*, Eindhoven 1967.
[3] J. F. Richardson, 'Fluidisation' (ed. J. F. Davidson and D. Harrison), Academic Press, London 1971, p. 26.
[4] V. G. Levich, 'Physiochemical Hydrodynamics', Prentice-Hall, New York, 1962, p. 90.
[5] R. Jottrand and F. Grunchard, 3rd Cong. Europ. Fed. Chem. Eng. London 1962, Session B p. 211.
[6] T. K. Ross and A. A. Wragg, *Electrochim. Acta*, **10**, (1965) 1093.
[7] D. C. Carbin and D. R. Gabe, *Electrochim. Acta*, **19**, (1974) 653.
[8] F. M. Brea and W. Hamilton, *Trans. Inst. Chem. Eng.*, **49**, (1971).
[9] G. J. V. Jagannadharaju and C. V. Rao, *Indian J. Tech.*, **3** (1965) 201.
[10] W. J. Beek, 'Fluidisation' (ed. J. F. Davidson and D. Harrison), Academic Press, London, 1971, p. 431.
[11] J. F. Richardson and W. N. Zaki, *Trans. Inst. Chem. Eng.*, **32** (1954), 35.
[12] W. K. Lewis, E. R. Gilliland and W. C. Bauer, *Ind. Eng. Chem.*, **41** (1949) 1104.